Arctic Ozone Amplifies Stratospheric Circulation Extremes

HAO-JHE HONG,[a,b] THOMAS REICHLER,[a] AND HUANG-HSIUNG HSU[b]

[a] *Department of Atmospheric Sciences, University of Utah, Salt Lake City, Utah*
[b] *Research Center for Environmental Changes, Academia Sinica, Taipei City, Taiwan*

(Manuscript received 7 August 2024, in final form 20 December 2024, accepted 10 February 2025)

ABSTRACT: Stratospheric ozone has long been suspected to drive interactions involving chemistry, radiation, and the circulation. However, the significance of these interactions, the underlying mechanisms, and the specific conditions that facilitate them remain poorly understood. In this study, we use a dry dynamical-core model with a simplified linear ozone scheme and a shortwave radiation parameterization to investigate these interactions. Our analysis, based on two long control simulations with either interactive or prescribed ozone, reveals that interactive ozone increases the persistence and interannual variability of the stratospheric circulation during northern spring, a period with sufficient solar radiation over the northern polar cap. This effect is closely linked to late-winter extreme stratospheric circulation events, such as stratospheric sudden warmings (SSWs) and vortex intensifications (VIs). While interactive ozone does not alter the frequency of these events, the ozone perturbations induced by the circulation amplify the associated temperature and wind anomalies. Specifically, late-winter VIs are followed by a colder and more persistent polar vortex in spring when interactive ozone is used, compared to fixed ozone. This results in a 5-day delay in the breakdown date of the vortex and a more positive North Atlantic Oscillation at the surface. Although interactive ozone also amplifies perturbations following SSWs, these effects are less pronounced than those observed for VIs. Our findings contribute to a growing body of evidence highlighting the importance of ozone–dynamics interactions for simulating the stratospheric circulation, its variability, and its surface impacts.

KEYWORDS: Stratospheric circulation; Climate prediction; Ozone

1. Introduction

Ozone is a key constituent of the stratosphere, essential for the complex interactions between chemistry, radiation, and dynamics (Hartmann 1981). Ozone absorbs solar radiation and thereby significantly influences the temperature and wind structure of the stratosphere (Cicerone 1987; Wallace and Hobbs 2006). Conversely, the distribution of ozone is strongly affected by stratospheric winds, particularly in the lower stratosphere (Butchart 2014; Tegtmeier et al. 2010). These mutual influences can lead to notable effects, especially during winter and spring, when stratospheric ozone can experience substantial perturbations. These perturbations may result from anthropogenic chemical depletion (Manney et al. 2011, 2020; Solomon 1999; Stolarski and Cicerone 1974) or dynamical transports linked to extreme stratospheric circulation events, such as stratospheric sudden warmings (SSWs) (Limpasuvan et al. 2004) and vortex intensification (VI) events (Limpasuvan et al. 2005). SSWs enhance the Brewer–Dobson circulation (BDC), increasing ozone transports into and concentrations in the lower stratosphere (Hong and Reichler 2021a; de la Cámara et al. 2018; Hocke et al. 2015; Lubis et al. 2017). VIs, on the other hand, cause opposite changes (Manney et al. 2011, 2020). However, VIs may be more important because they can lead to an additional ozone reducing process: The cooling of the polar vortex during VIs creates favorable conditions for ozone depletion by heterogeneous chemical processes (Tegtmeier et al. 2008). SSWs do not exhibit a similar opposite chemical effect.

The important role that stratospheric ozone plays in the circulation was first recognized over the high latitudes of the Southern Hemisphere. Early studies focused on the effects of Antarctic stratospheric ozone depletion and found that the declining trend of ozone was accompanied by stratospheric cooling and an intensification of the polar circulation that extended from the stratosphere to the troposphere (Randel and Wu 1999; Thompson and Solomon 2002; Gillett and Thompson 2003).

In the Arctic stratosphere, understanding the interactions between ozone and the circulation is more complicated due to the large internal variability of the circulation and the induced transport dynamics on polar ozone (Harzer et al. 2023). The upward propagation and dissipation of planetary waves modulate the strength of the northern wintertime stratospheric polar vortex (Limpasuvan et al. 2004, 2005), which—through anomalous mixing and transports—changes the amount and distribution of polar ozone. Ozone, in turn, and especially zonal asymmetries in the distribution of ozone and the resulting radiative heating anomalies, can change the planetary waves and how they propagate and break (Gabriel et al. 2007; Nathan and Cordero 2007). These and other processes can create complicated situations, and most often complex Chemistry–Climate Models (CCMs) are used to study the interactions between ozone and the circulation.

However, most models from the Coupled Model Intercomparison Project use prescribed climatological means of ozone to represent the approximate radiative effects of ozone and to avoid the large computational burden from the chemistry

Supplemental information related to this paper is available at the Journals Online website: https://doi.org/10.1175/JCLI-D-24-0446.s1.

Corresponding author: Thomas Reichler, thomas.reichler@utah.edu

DOI: 10.1175/JCLI-D-24-0446.1

components (Keeble et al. 2021). Prescribing ozone in models, however, inhibits the interaction between ozone and the circulation, leads to inconsistencies between the two, and may create simulation errors (Ivanciu et al. 2021). To understand these errors and to find out whether interactive ozone leads to more reliable simulations, past studies compared simulations in which ozone was either interactively simulated or prescribed.

For the Southern Hemisphere, it was found that using interactive ozone increases the circulation effects from Antarctic ozone depletion (Haase et al. 2020; Ivanciu et al. 2021; Li et al. 2016). Analyzing CMIP6 model output, Revell et al. (2022) found that models without interactive chemistry project a substantially stronger tropospheric westerly jet by the end of the twenty-first century than models with interactive chemistry because the prescribed ozone recovery is smaller than the predicted one.

For the Northern Hemisphere, several recent studies have demonstrated the significance of interactive stratospheric ozone for simulating Arctic circulation and surface conditions. Rae et al. (2019) showed that simulations with dynamically consistent ozone produce a polar vortex shape and sea level pressure pattern that more closely resemble those from a full CCM compared to simulations with fixed ozone. Haase and Matthes (2019) found that interactive ozone results in more realistic and persistent circulation anomalies in the stratosphere and at the surface after SSWs compared to prescribed ozone. Romanowsky et al. (2019) observed that in response to sea ice retreat, the coupling between the stratosphere and troposphere is more intense with an interactive ozone scheme. Rieder et al. (2019) demonstrated that interactive ozone chemistry increases simulated stratospheric temperature variability and extremes. Friedel et al. (2022) found that the interaction between ozone and the stratospheric circulation results in a more variable timing for the breakdown of the Arctic polar vortex during spring.

In the present study, we also investigate the effects of interactive ozone on Arctic circulation and surface conditions. Unlike previous studies with complex CCMs, we employ a relatively simple idealized general circulation model with dry physics. By coupling this model with an ozone scheme and implementing a basic shortwave radiation parameterization, we reproduce the fundamental mechanisms governing the interaction between ozone and dynamics. This approach has several advantages. First, our model avoids the complexities and parameterizations found in more comprehensive models, focusing on the essential physical processes (Held 2005). This simplification allows for a clearer analysis of the interactions between ozone and dynamics. Additionally, the model's computational efficiency and ease of management make it a valuable research tool, offering a fresh perspective on understanding ozone–dynamics interactions and providing a foundation for future investigations.

We employ the simplified linear ozone scheme by Cariolle and Teyssèdre (2007) in our model. Variations of this scheme are used in other atmospheric models, including the ECMWF Integrated Forecasting System (IFS) (Monge-Sanz et al. 2022), the NCEP Twentieth Century Reanalysis (20CR) (Compo et al. 2011), the NCEP Global Forecast System (GFS), and the NCEP Climate Forecast System, version 2 (CFSv2) (Saha et al. 2014; McCormack et al. 2006). As such, the results from our study can also serve as a test of the performance of this widely used ozone model.

The main goal of this study is to better understand the influence of interactive ozone on Arctic stratospheric circulation and surface conditions. We also aim to compare how these influences are simulated by our idealized model with those simulated by full CCMs. A particular focus is on Arctic stratospheric circulation extremes, such as SSWs and VIs, as these events are known to be associated with significant perturbations in stratospheric polar ozone (Hong and Reichler 2021a). To ensure that these ozone perturbations are dynamically relevant, we focus on circulation extremes that occur in late northern winter (February–March) and persist into northern spring. This period is critical because there is sufficient sunlight over the polar cap for ozone to generate radiative heating anomalies.

Our paper is structured as follows: Section 2 describes our model and methodology; section 3 presents our results, focusing on the impact of interactive ozone on Arctic circulation variability; and section 4 provides a summary and conclusions.

2. Model and methods

a. *The SCDM*

We employ the Simplified Chemistry–Dynamical Model (SCDM V1.0), developed by Hong and Reichler (2021b). SCDM is based on the GFDL spectral dynamical core (Held and Suarez 1994) with simplified physics. Modifications were made according to Wu and Reichler (2018), incorporating realistic topography and forcing the model with empirically derived, zonally asymmetric, and seasonally varying equilibrium temperatures, based on the 1980–2020 temperature climatology from the MERRA-2 reanalysis (Bosilovich et al. 2015). This minimizes the climatological temperature differences between the reanalysis and the model, resulting in effective diabatic heating rates that reasonably match observations. The model successfully captures seasonal variations in stationary waves, polar vortex strength, and SSW frequency, validating its use for our study.

Hong and Reichler (2021b) improved the model by adding ozone as a tracer advected by the dynamics and implementing the photochemical ozone scheme by Cariolle and Teyssèdre (2007). The scheme linearly approximates ozone tendencies with respect to photochemical equilibrium for the local values of the ozone mixing ratio, temperature, and overhead column ozone. The scheme also includes an additional term for ozone destruction by heterogeneous chemistry with a peak chlorine value of 3.6 ppbv in the upper stratosphere. Further, Hong and Reichler (2021b) implemented into the SCDM a shortwave radiation parameterization for ozone (Lacis and Hansen 1974) to simulate the interactions between dynamics and ozone in the stratosphere.

We conducted two 2000-yr simulations with the model. VARO3 is our control run with variable, fully interactive ozone. FIXO3 is identical to VARO3, except that ozone is prescribed using the fixed, zonally asymmetric, daily varying but annually repeating ozone climatology derived from VARO3. The differences

between the two simulations are, therefore, entirely due to the mutual influences between the dynamics and ozone.

b. Methods

1) PERSISTENCE OF THE NORTHERN ANNULAR MODE

We followed Kim and Reichler (2016) to estimate the persistence time scale τ of the Northern Annular Mode (NAM) index, represented at each level by the standardized geopotential height anomalies averaged over the polar cap area (60°–90°N). The τ is defined as the time in which the daily autocorrelation of the NAM index decreases by a factor of e. To calculate the mean and variability of τ, we divided the 2000-yr dataset into forty 50-yr intervals and calculated τ separately for each interval. This process was repeated for each latitude, level, and calendar day. A two-sample Student's t test was used to test the significance of the differences in τ between VARO3 and FIXO3.

2) STRATOSPHERIC CIRCULATION EVENTS

Ozone in the stratosphere is well known to be influenced by the anomalous advection and temperatures during the life cycles of stratospheric circulation events. The two types of events we consider are SSWs and VIs. SSWs are characterized by a relatively warm and weak northern wintertime stratospheric polar vortex, while VIs are characterized by a relatively cold and strong vortex.

We defined SSWs based on Charlton and Polvani (2007). According to this definition, the central or onset date of an SSW is the day when the zonal-mean zonal wind at 10 hPa and 60°N (U1060) reverses from westerly to easterly between November and March. After the wind reversal, U1060 must return to westerly for at least 10 consecutive days before the end of April; otherwise, the event is classified as a final warming (FW) event. If two SSWs occur in the same winter, a period of at least 20 consecutive days of westerlies is required to distinguish the two events.

For VIs, we followed the definition by Hong and Reichler (2021a). This definition is based on daily anomalies of U1060, low-pass filtered using a 20-day running mean. The central date of a VI is defined when the filtered U1060 anomaly exceeds 16 m s^{-1}, which is about one standard deviation of U1060 estimated from reanalysis. The VI onset date is the day of maximum U1060 within 30 days after the threshold is exceeded. Similar to SSWs, a separation interval of at least 20 days is required for two VIs occurring in the same winter to be recognized as separate events.

We only considered events occurring in February and March, as this is when sufficient sunlight is available over the polar cap for ozone to create shortwave radiative heating and thus provide a radiative feedback on the circulation. For the 2000-yr-long VARO3 (FIXO3) simulation, this resulted in 830 (821) SSW events and 449 (445) VI events (Table 1). All other years were considered normal years. Table 1 further shows that the number of events that occur during any month, i.e., not just during February or March, is almost identical between the two simulations. However, there are some differences between VARO3 and FIXO3 in how the events are distributed between the individual months (Fig. S1 in the online supplemental material). During November–January, these differences are usually small. However, during the other months, ozone causes small but significant variations in event frequency: in February, VARO3 has somewhat more SSWs and VIs than FIXO3, resulting in fewer events in March. There are also more VIs in April and more FWs in May in VARO3.

TABLE 1. Statistics of SSWs and VIs that occur during (top) November–March and (bottom) February–March. Listed are the number of events (No.), mean onset date (onset), mean FW date following the event (FW), and time in days between onset and FW (d). The mean FW date for all years is 4/15 (ERA5), 4/5 (VARO3), and 4/4 (FIXO3). The standard deviation of the FW date for VARO3 and FIXO3 varies between 14 and 19 days. Asterisks (*) indicate that the difference in mean FW date between VARO3 and FIXO3 is significant at the 5% level based on a two-sample t test.

	No.	Onset	FW	d
		SSW (November–March)		
ERA5	27	2/2	4/23	80
VARO3	1375	2/4	4/6	61
FIXO3	1374	2/5	4/6	60
		SSW (February–March)		
ERA5	15	2/26	4/23	56
VARO3	830	2/23	4/9	45
FIXO3	821	2/24	4/9	44
		VI (November–March)		
ERA5	11	1/23	4/5	72
VARO3	970	1/26	4/10	74
FIXO3	1015	1/27	4/7	70
		VI (February–March)		
ERA5	7	2/27	4/17	49
VARO3	449	2/23	4/16	52*
FIXO3	445	2/25	4/11	45*

As these differences are relatively small, we conclude that using interactive chemistry in our model leads only to small changes in the number of extreme circulation events. This contrasts with a similar CCM-based study by Haase and Matthes (2019), who found that compared to prescribed ozone, interactive ozone leads to significant changes in the overall frequency of SSWs and their seasonal distribution. These differences could be due to ozone's longwave radiative effects, which may alter the stratospheric background year-round, including polar night. Haase and Matthes (2019) CCM simulates these effects, but not our model.

3) EVENT COMPOSITING

We formed composites of all February–March events by focusing on the interval from −90 to 90 days centered on the onset date of each event and then averaging over all events. A one-sample t test was used to determine whether the composite anomalies were significant, and a two-sample t test was used to assess the significance of composite difference anomalies.

3. Results

In this section, we investigate the impact of interactive ozone by comparing the two simulations. We begin by exploring the

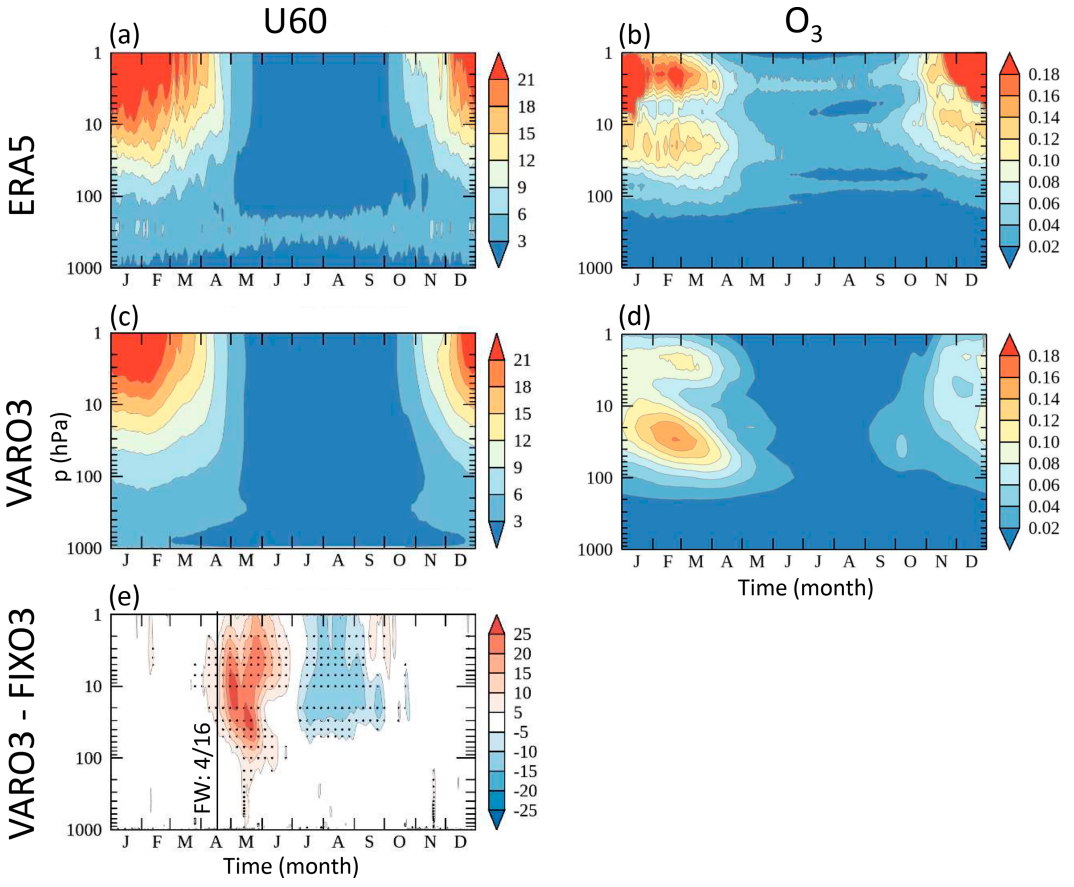

FIG. 1. Interannual variability of (left) zonal-mean zonal wind at 60°N (U60) (m s^{-1}) and (right) polar cap–averaged (60°–90°N) ozone volume mixing ratio (ppmv). (a),(b) ERA5 (1979–2020), (c),(d) VARO3 (interactive ozone), and (e) VARO3 minus FIXO3 (interactive ozone minus fixed ozone; U60 only). The interannual variability is the year-to-year standard deviation on any given day of the year. Stippling in (e) indicates statistically significant differences at the 5% level based on an *F* test. The vertical line in (e) highlights 16 Apr, the mean onset date of FWs that follow VIs in VARO3.

circulation variability, followed by an examination of specific changes in ozone, ozone heating, and the circulation associated with the two event types. Finally, we assess whether the stratospheric changes translate into observable signals at the surface. As mentioned before, we focus on events during boreal spring (February–March), as this is when the signals are most pronounced.

a. Changes in circulation variability

An interaction between ozone and the dynamics should be evident through changes in stratospheric variability. This interaction can result in either constructive or destructive interference between the initial perturbations and the additional response from interactive ozone. Constructive interference would amplify the initial perturbations, increase variability, and potentially create a positive feedback loop; otherwise, the initial perturbations will be dampened, leading to decreased variability. To investigate these possibilities, we examine the interannual standard deviation of the zonal-mean zonal wind at 60°N (U60), a common measure of the Arctic polar vortex strength. The standard deviation is calculated for each calendar date and atmospheric level.

The top two panels in Fig. 1 compare the variability between the fifth generation ECMWF atmospheric reanalysis (ERA5, 1979–2000) (Hersbach et al. 2020) and VARO3 in terms of (left) U60 and (right) ozone. Generally, the variability of the polar vortex in ERA5 is large in winter and small in summer, and this is well simulated by VARO3. VARO3 also replicates the ERA5 variability structure of the Antarctic polar vortex at 60°S quite well (Fig. S2). VARO3 simulates the ERA5 ozone variability in the lower stratosphere reasonably well, but the model has much smaller variability than ERA5 in the upper half. This discrepancy could be due to very large and unrealistic amounts of ERA5 ozone in the high stratosphere during the 1980s and 1990s in polar night (Hersbach et al. 2018).

Next, we compare simulations VARO3 and FIXO3 to investigate the impact of interactive ozone on circulation variability. Figure 1c shows the difference in U60 variability between the two simulations. As expected, the differences are

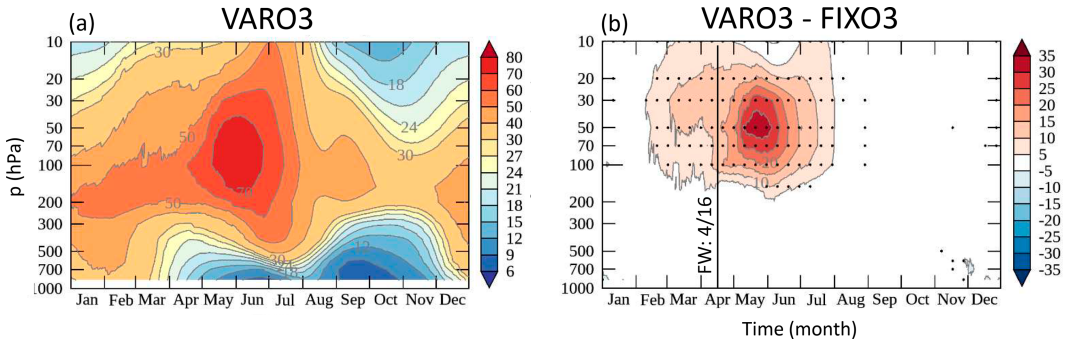

FIG. 2. Persistence time scale τ (days) of the NAM index for (a) VARO3 and (b) VARO3 minus FIXO3. Stippling in (b) indicates statistically significant differences at the 5% level. The vertical line in (b) highlights 16 Apr, the mean onset date of FWs that follow VIs in VARO3.

mostly small during winter (November–March), as ozone's influence on the polar stratosphere is linked to the presence of sufficient sunlight. However, starting in April and continuing into May, Fig. 1c reveals a 20%–25% increase in circulation variability in VARO3 compared to FIXO3. During boreal summer, interactive ozone decreases stratospheric variability. However, this change is relatively small, as it coincides with the natural low variability during this time of the year. Therefore, for the remainder of this paper, we focus on understanding the reasons for and consequences of the increase in variability during boreal spring.

This increase in variability in VARO3 during spring is consistent with constructive interference between the stratospheric dynamics and Arctic ozone, occurring when there is sufficient sunlight for stratospheric ozone perturbations to induce radiative heating anomalies that, in turn, influence the circulation. Our results align with those of Rieder et al. (2019), who found from a complex CCM that stratospheric temperature variability and temperature extremes during spring are increased in simulations with interactive chemistry compared to simulations with fixed climatological mean ozone.

To better understand the nature of the increased interannual circulation variability due to interactive ozone, we next examine the NAM persistence time scale τ. Figure 2a shows a pronounced springtime maximum in τ for VARO3, reaching up to 70 days in the lower stratosphere (100–50 hPa) during May and June. From observations and more complex models, Kim and Reichler (2016) found a similar but less pronounced increase in τ, reaching about 40 days during spring in the lower stratosphere.

Next, we compare τ from VARO3 against that from FIXO3 (Fig. 2b). The differences demonstrate that using interactive ozone makes the stratospheric NAM, and thus the polar vortex, more persistent compared to using fixed ozone. The increase in τ of about 10–30 days extends from February to July and maximizes in the lower stratosphere during May and June, coinciding with the time and level where persistence is highest in VARO3 (Fig. 2a). The delay between the maximum response in interannual vortex variability (Fig. 1c) and NAM persistence (Fig. 2b) likely reflects the persistence of vortex perturbations caused by prior ozone perturbations.

b. *Changes in ozone during stratospheric circulation events*

Previous studies have shown that SSWs and VIs, the major stratospheric circulation events, are associated with persistent anomalies in stratospheric ozone that can last for up to 2 months (de la Cámara et al. 2018; Hocke et al. 2015; Hong and Reichler 2021a). Therefore, we focus next on the ozone perturbations simulated by our model during these events.

The thin curves in Figs. 3a and 3b represent individual annual time series (October–September) of the polar cap–averaged ozone mixing ratio at 70 hPa for (left) ERA5 and (right) the first hundred years of VARO3. The color coding indicates whether an SSW, VI, or no circulation event occurred during each period. Consistent with previous studies, the dynamical transports associated with SSWs lead to increased amounts of ozone from January to April compared to neutral years, while VIs result in larger and more persistent decreases in ozone. This can also be seen from the thick curves in Figs. 3a and 3b, which show the evolution of ozone averaged over the events from all simulated years. VARO3 simulates the seasonality and event differences of ozone well, but as noted in Hong and Reichler (2021b), ozone at 70 hPa is positively biased by about 30% compared to ERA5.

The remaining panels of Fig. 3 illustrate the spatial structure of February–April mean ozone anomalies in latitude–height cross sections for SSW and VI years, respectively, based on all years of ERA5 and VARO3. In ERA5, increased ozone during SSWs and decreased ozone during VIs maximize at ~10 hPa near the pole, whereas in VARO3, the peak is at ~40 hPa. During VIs, the magnitude of the ozone anomalies in both ERA5 and VARO3 is approximately 2–3 times larger compared to those during SSWs. As discussed in the introduction, the more pronounced VI-related ozone anomalies may stem from additional ozone depletion caused by heterogeneous chemistry, which is absent during SSWs.

c. *Changes in final warming date*

Friedel et al. (2022) demonstrated that reductions in ozone during strong and cold vortex events (VIs) result in decreased solar absorption, more persistent cold anomalies in the lower stratosphere, and a stronger and more enduring polar vortex

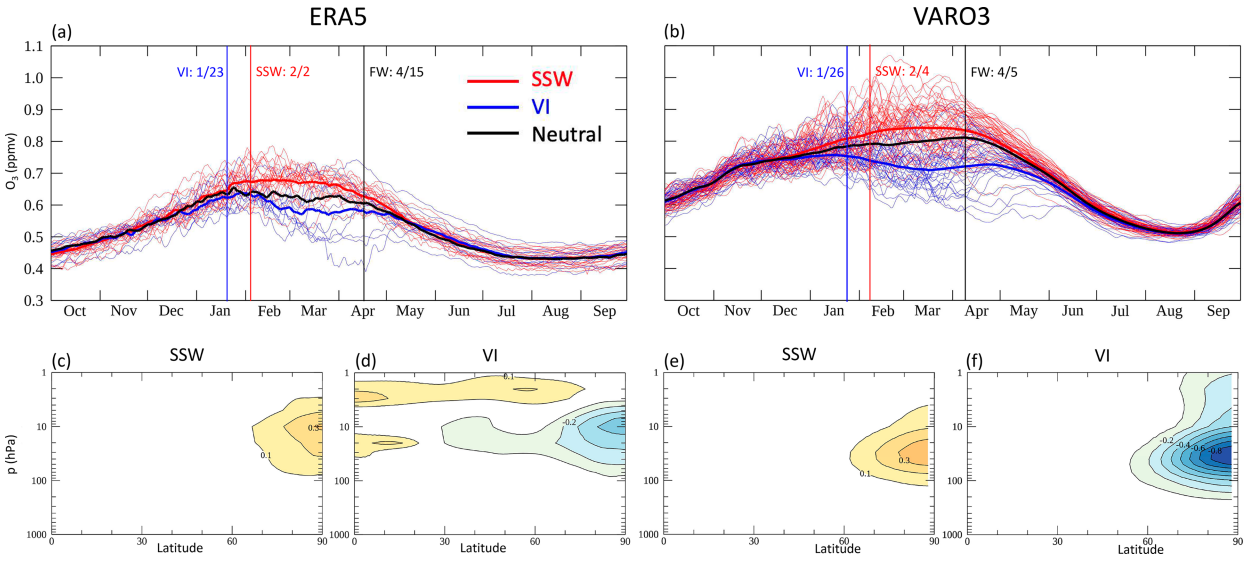

FIG. 3. Ozone during stratospheric circulation events in (left) ERA5 and (right) VARO3. (top) Time series of northern polar cap (60°–90°N)–averaged ozone volume mixing ratio at 70 hPa during SSWs (red), VIs (blue), and neutral years (black) during any time of the winter; thick curves are means over the entire period; thin curves show individual years; for clarity, for VARO3 only the first 100 years are included. Vertical lines show the mean onset date for VIs, SSWs, and FWs. (bottom) Spatial structure of composite ozone anomalies for years with February–March (c),(e) SSWs and (d),(f) VIs; the latitude–height cross sections show zonal-mean ozone volume mixing ratio anomalies averaged from February to April.

and NAM. Consequently, the breakup of the spring polar vortex, known as the FW, is significantly delayed by up to 10 days compared to simulations with fixed climatological ozone. We will next investigate whether similar changes in the seasonal timing of the FW are observed in our simulations and whether SSWs have the anticipated opposite effect.

We classified FWs based on whether they were preceded by stratospheric circulation events during February–March. We then calculated the mean date of FWs following SSWs and VIs for both the VARO3 and FIXO3 simulations (Table 1). Consistent with the findings of Friedel et al. (2022), the VARO3 simulation shows that FWs following VIs (16 April) are, on average, significantly delayed by 5 days compared to those in the FIXO3 simulation (11 April). This delay is consistent with the negative ozone anomalies associated with VIs (Fig. 3). As we will show later, this results in a stronger, colder, and more persistent polar vortex, which requires more wave fluxes and more shortwave radiative heating to break down.

The situation is different for FWs that follow SSWs. They occur, on average, on 9 April compared to the 5 April mean date of all FWs (Table 1). This 4-day delay is a consequence of the overrecovery of the vortex that typically follows SSWs (Hu et al. 2014; Rupp et al. 2023), and it is similar between VARO3 and FIXO3, possibly because the ozone anomalies during SSWs are weaker than during VIs (Fig. 3). Additionally, VARO3 results in a somewhat greater variability in the FW date compared to FIXO3 (not shown). Overall, our results corroborate previous studies by demonstrating that interactive ozone leads to a more persistent polar vortex and a later FW date when preceded by a VI. This outcome further validates our model's ability to effectively simulate the interactions between ozone and stratospheric dynamics.

d. *Interactions between ozone and the stratospheric circulation*

In the previous sections, we demonstrated how late-winter (February–March) SSWs and VIs are associated with distinct anomalies in springtime Arctic ozone. We now aim to explore the dynamical consequences of these anomalies by examining their spatiotemporal evolution and their radiative impacts. As before, our analysis focuses on years with VIs or SSWs occurring during February–March, a period when sunlight is available over the polar cap to drive significant radiative effects.

Figure 4 illustrates the composite anomalies in ozone (top and middle) and the associated ozone shortwave heating rate for VARO3 (bottom). The ERA5 ozone changes during SSWs (Fig. 4a) are well simulated by the model (Fig. 4c). The rapid increase in ozone following the onset is driven by the upward propagation and breaking of planetary waves prior to SSW onset (Fig. S3), which weakens the stratospheric polar vortex, accelerates the downwelling branch of the BDC, and results in the anomalous transport of ozone-rich air from the tropical upper stratosphere into the Arctic lower stratosphere (de la Cámara et al. 2018; Hong and Reichler 2021a). This ozone increase creates persistent shortwave heating anomalies in the lower stratosphere and smaller cooling anomalies above (Fig. 4e), similar to a previous study using a CCM (Oehrlein et al. 2020, their Fig. 5d).

The right panels of Fig. 4 illustrate anomalies associated with VIs. Before onset, planetary wave activity is reduced (Fig. S3), creating a weaker BDC and less ozone transport

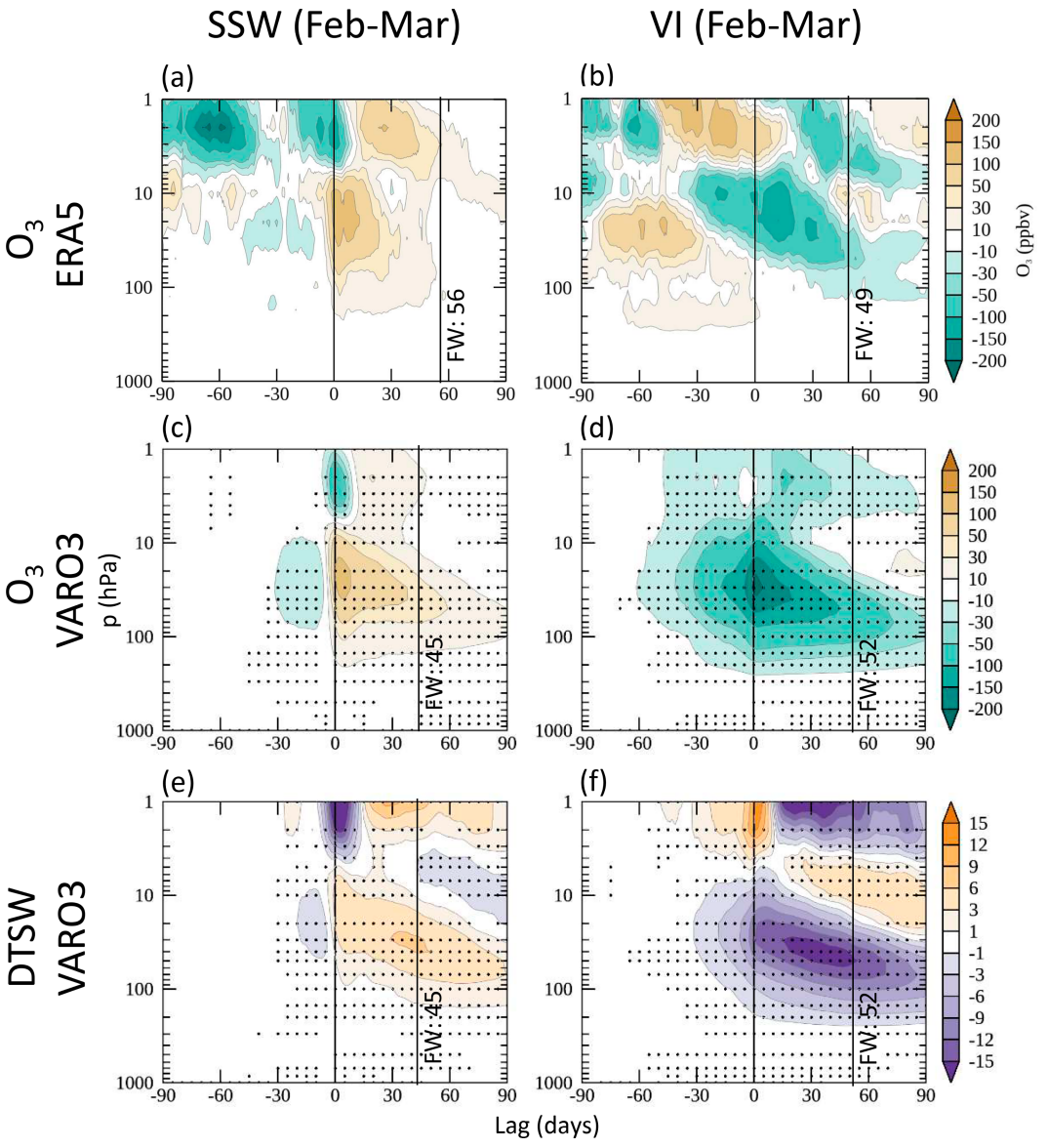

FIG. 4. Composite anomalies during SSWs and VIs. (top) ERA5 ozone (polar cap–averaged 60°–90°N volume mixing ratio in ppbv), (middle) VARO3 ozone, and (bottom) VARO3 shortwave heating rate (DTSW) (10^{-3} K day^{-1}). Only February and March events are included, leading to 15 SSWs and 7 VIs for ERA5, and 830 SSWs and 449 VIs for VARO3. Vertical lines indicate event onset and mean FW date. Stippling indicates statistically significant anomalies at the 5% level. The ERA5 anomalies are insignificant due to the small number of events.

into the Arctic stratosphere. At the same time, the cold vortex creates favorable conditions for catalytic ozone depletion. Starting about 60–30 days before onset, persistent negative ozone anomalies occur in ERA5 (Fig. 4b) and VARO3 (Fig. 4d). These lead to radiative cooling anomalies in the lower stratosphere (Fig. 4f), which start at event onset, last for more than 60 days, and are stronger than the heating anomalies observed during SSWs (Fig. 4e).

Compared to ERA5, the SCDM ozone simulations during circulation events are reasonable, except that the anomalies are shifted downward, more persistent, and stronger than in ERA5. Possible reasons include model shortcomings in simulating wave activity changes after the circulation events (Hong and Reichler 2021b). However, the primary purpose of our study is to qualitatively understand the ozone–dynamics feedback, and the SCDM's reasonable ozone response justifies its use for this study.

Next, we investigate how the changes in ozone and heating seen in Fig. 4 influence temperatures and the circulation. Figure 5 shows composite anomalies of Arctic temperatures during SSWs and VIs. During SSWs, the ERA5 temperatures exhibit a warming center at 10 hPa with a downward propagating

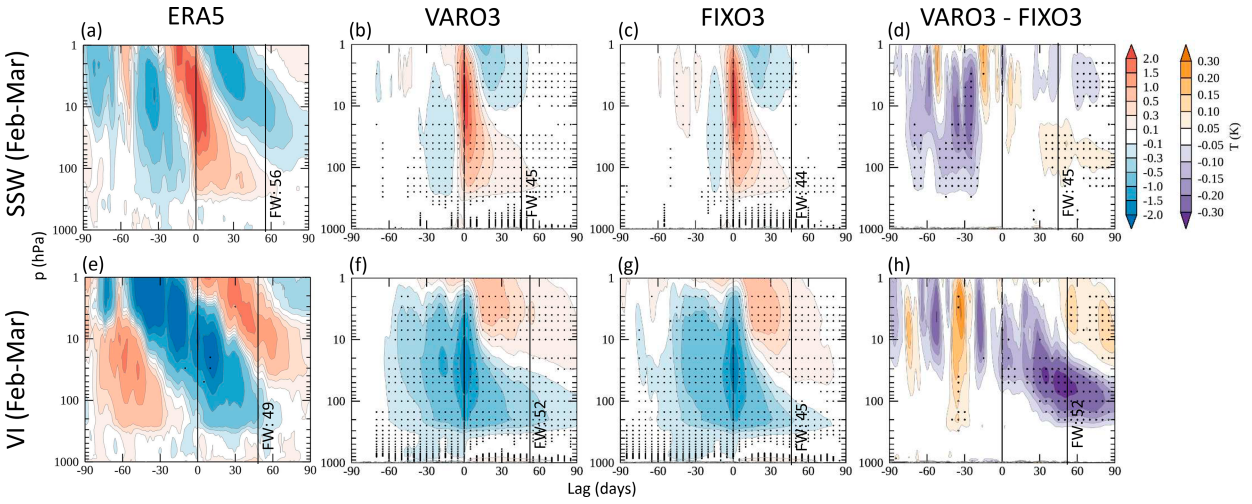

FIG. 5. Temperature response to stratospheric events. Shown are composite anomalies of polar cap (60°–90°N)–averaged temperature (K) for February–March (top) SSWs and (bottom) VIs. Data are from (a),(e) ERA5, (b),(f) VARO3, (c),(g) FIXO3, and (d),(h) VARO3 minus FIXO3. Vertical lines indicate event onset and mean FW date for ERA5 and VARO3. (a)–(c) Stippling represents statistically significant (e)–(g) anomalies and (d),(h) anomaly differences at the 5% level. The ERA5 anomalies are insignificant due to the small number of events.

structure (Fig. 5a), which is also simulated by VARO3—albeit at weaker amplitudes. As with ozone, this warming is primarily a consequence of the intensified downwelling branch of the BDC during SSWs and the associated adiabatic warming.

Compared to VARO3, the SSW-related warming of FIXO3 (Fig. 5c) is somewhat weaker and less persistent. This can be more clearly seen from the difference plot in Fig. 5d. VARO3 shows a small (0.05–0.1 K) but significant warming difference in the lower stratosphere 30–90 days after onset, consistent with the increase in ozone shortwave heating (Fig. 4). The timing of the warming difference is somewhat delayed with respect to the time of the maximum ozone heating (Fig. 4e), reflecting the thermal inertia of the atmosphere. VARO3 and FIXO3 also show some robust and statistically significant temperature differences before the onset date, a point to which we come back later in our discussion.

In contrast to SSWs, VIs are associated with a weaker BDC, less adiabatic warming, and cooling (Figs. 5e–g). Compared to the warming during SSWs, the cooling has a much broader and more persistent structure, in particular in the ERA5, reflecting dynamical differences between the two opposing circulation events. VIs are associated with gradual and long-lasting reductions in planetary wave activity that start long before the onset date, and slight but sudden increases after (Figs. S3d and S3e) (Hong and Reichler 2021a). These lead to broader signals than SSWs.

Comparing VARO3 and FIXO3 during VIs, interactive ozone enhances the amplitude and persistence of the cooling, which can be better seen from the differences in cooling in Fig. 5h. As expected from the differences in shortwave heating (Fig. 4f), there is a rather strong (from −0.2 to −0.3 K) and significant additional cooling in VARO3 compared to FIXO3, mostly after onset. This cooling is about 3–6 times larger than the heating during SSWs (Fig. 5d), consistent with the stronger ozone perturbations during VIs (Fig. 4f).

We next discuss how interactive ozone modulates the response of U60, the zonal-mean zonal wind at 60°N, to SSWs and VIs (Fig. 6). The U60 (or vortex) weakening in the aftermath of SSWs (Fig. 6a) is simulated by the SCDM (Figs. 6b,c), but is weaker, less persistent, and descends less downward than in the ERA5. The difference between VARO3 and FIXO3 (Fig. 6d) shows additional weakening from ozone from day 30 to 90, coexistent with the additional polar cap warming seen in Fig. 5d, and dynamically consistent with the thermal wind relationship and the reduction of the meridional temperature gradient by the extra heating. Compared to the mean reduction in vortex strength at day 30 after SSWs (~3 m s^{-1}), the magnitude of this ozone-related extra vortex weakening is quite sizable (~1 m s^{-1}). An analogous structure of weakening U60 after SSWs caused by interactive ozone has been shown by the CCM study of Haase and Matthes (2019, their Fig. 8), reinforcing the findings from our simulations.

During VIs, the ERA5 shows a descending U60 strengthening, flanked by a weakening both long before and long after the event (Fig. 6e). The strengthening is quite well simulated by the model (Figs. 6f,g), with interactive ozone amplifying it (Fig. 6h). There are no negative U60 anomalies before and after the event as in ERA5.

Since the extra cooling after VIs is larger (Fig. 5h) than the warming after SSWs (Fig. 5d), the thermal wind relationship predicts that the circulation change from interactive ozone must also be larger for VIs than for SSWs. This is confirmed by comparing Fig. 6h with Fig. 6d. According to Fig. 6h, the ozone-induced wind anomalies emerge right after VI onset (23 February), maximize 30–52 days after (24 March–16 April), and quickly disperse after the FW on day 52 (16 April). Interestingly, the strongest wind anomalies occur just a few days after the March

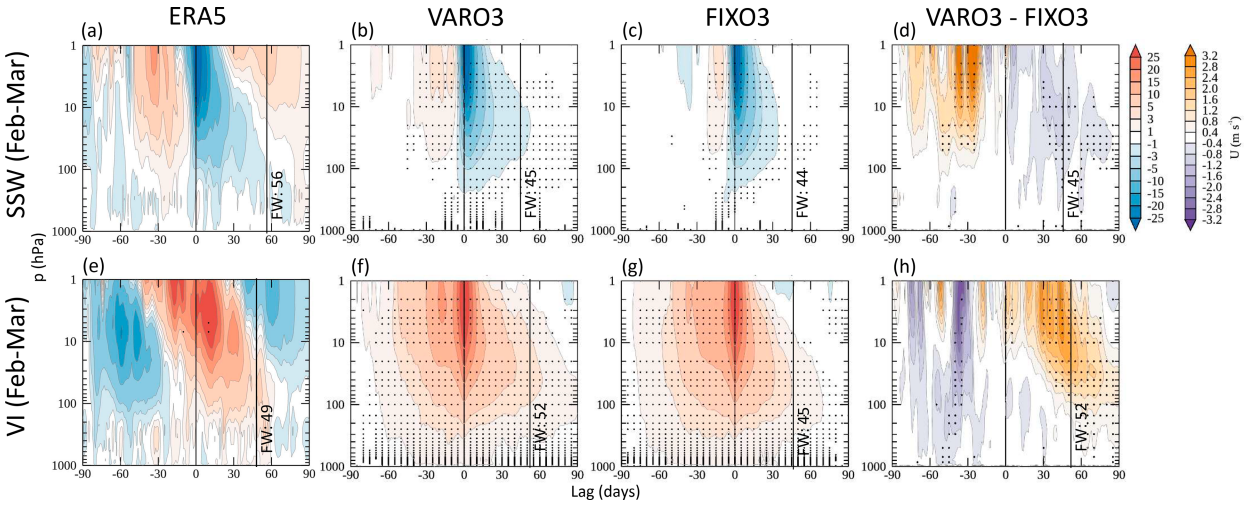

FIG. 6. As in Fig. 5, but for zonal-mean zonal wind at 60°N (U60) (m s^{-1}).

equinox, i.e., the start of polar day over the pole. It is plausible that the ozone-related extra strengthening of the vortex following VIs creates the previously shown 5-day delay in the mean breakup date of the polar vortex (Table 1). An ozone effect on the vortex breakup date after SSWs cannot be detected, likely because during SSWs, the ozone influence on the vortex is rather weak.

Some previous CCM studies described a negative feedback between the dynamics and ozone in the stratosphere (Lin et al. 2017; Haase and Matthes 2019). This feedback involves the modulation of upward propagating planetary waves by the varying atmospheric background winds (Charney and Drazin 1961). For example, an initial strengthening of the polar vortex (e.g., from ozone depletion) would increase the westerly background winds and, if the winds are not too strong, favor the planetary wave propagation upward. This would weaken the polar vortex, intensify the BDC, transport more ozone into the polar regions, and overall counteract the initial reasons for the changes. Hence, this would be a negative feedback.

Haase and Matthes (2019) found that using interactive ozone in a CCM strengthens the polar vortex in early winter and spring, and that the spring strengthening is connected to a negative feedback mechanism. In contrast, our study finds that the effects of interactive ozone outside the spring season are negligibly small (Figs. 1 and 2), and that interactive ozone during spring amplifies the polar vortex anomalies. Our study does not support the relevance of this negative feedback for stratospheric dynamics, but this may be due to our model's shortcomings, like the aforementioned simulation of wave activity changes after circulation events.

We investigated whether we could at least identify some elements of this negative feedback in our simulations. As shown in Figs. S3d and S3e, VI events are followed by an increase in upward planetary wave propagation, indicated by the positive anomaly of the vertical component of the Eliassen–Palm flux. The difference between VARO3 and FIXO3 (Fig. S3f) is quite noisy but shows an anomaly difference that is generally somewhat negative, suggesting that interactive ozone slightly reduces the upward wave propagation after VIs. Although these changes are not statistically significant, they would further decrease the strength of the BDC and result in a positive feedback.

There are several possible reasons for why we are unable to detect this negative feedback. For example, Haase and Matthes (2019) based their study on climatological (monthly) mean values and focused on the influence of spring ozone depletion on the dynamics of the vortex breakdown. Our study, on the other hand, focused on late-winter extreme stratospheric circulation events and the anomalies that follow. Additionally, for the negative feedback to work, the background winds must be weak, a condition that usually holds in spring before the vortex breaks down. It is, however, questionable whether this is also true in our case, because VIs are followed by relatively strong westerlies (Fig. 6).

e. *Surface impacts*

It is well known that the dynamical interaction of the stratospheric polar vortex with the tropospheric circulation affects the surface, particularly over the North Atlantic (Baldwin and Dunkerton 2001; Kidston et al. 2015). Specifically, SSWs are associated with a more negative phase of the North Atlantic Oscillation (NAO), while VIs are linked to a more positive NAO phase. The more practical question to be addressed in this section is whether the ozone-induced additional perturbations of the polar vortex are strong enough to cause detectable impacts at the surface, or in other words, whether interactive ozone matters for the simulation and prediction of tropospheric weather and climate.

Our analysis focuses on changes in sea level pressure (SLP) because, in this idealized model, this is the most meaningful surface quantity. Figure 7 presents time-mean SLP anomaly composites for the February–March stratospheric circulation events discussed previously. The selected time-mean interval spans from day 30 to 90 after event onset, capturing the period of maximum stratospheric circulation anomalies induced by interactive ozone (see Figs. 6d,h).

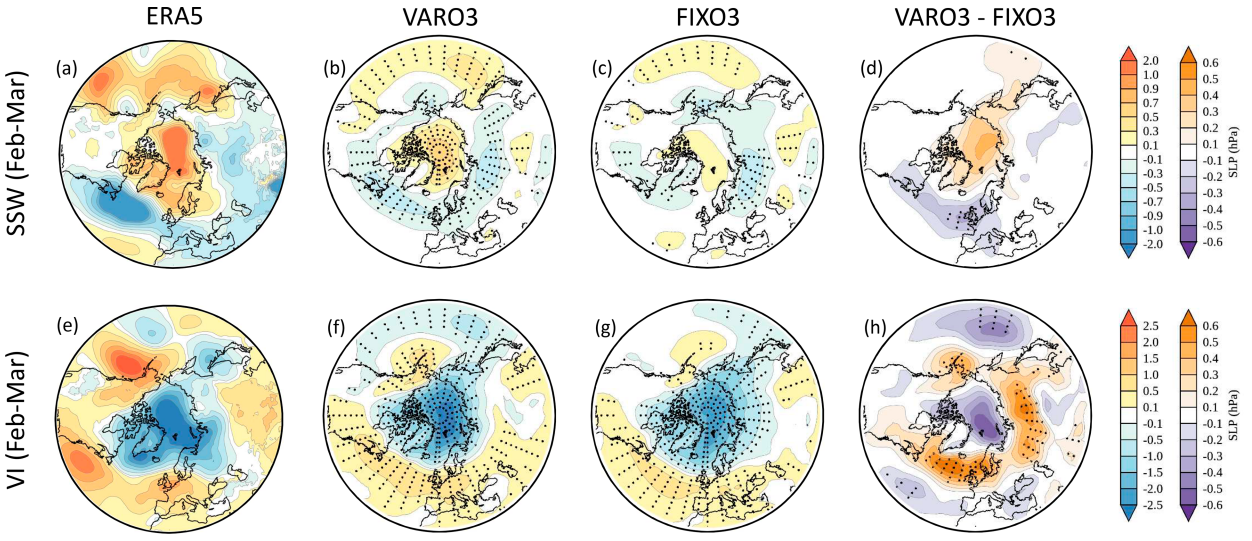

FIG. 7. SLP response to stratospheric events. Shown are composite SLP anomalies averaged from lag 30 to 90 days with respect to the onset of (top) SSWs and (bottom) VIs that occur during February–March. Data are from (a),(e) ERA5, (b),(f) VARO3, (c),(g) FIXO3, and (d),(h) VARO3 minus FIXO3. (a)–(c) Stippling represents statistically significant (e)–(g) anomalies and (d),(h) anomaly differences at the 5% level. The ERA5 anomalies are insignificant due to the small number of events.

SSWs are followed by a negative NAO over the North Atlantic, which is weaker in the model (Figs. 7b,c) than in ERA5. This is likely due to the simplified nature of our model, leaving it unable to reproduce the vortex weakening and the downward descent of the wind anomalies into the troposphere at its full strength (Figs. 6a–c). Nevertheless, the negative NAO after SSWs is clearer in VARO3 than in FIXO3, likely because of the additional shortwave heating from interactive ozone, amplifying and extending the lifetime of the SSW perturbations in the stratosphere, and thereby increasing their downward effect onto the surface. This can be most clearly seen from the difference between VARO3 and FIXO3 (Fig. 7d). The more pronounced negative NAO from ozone is also consistent with previous studies using full CCMs (Haase and Matthes, 2019; Oehrlein et al. 2020).

VIs are followed by a positive NAO (Figs. 7e–g), with SLP magnitudes that are generally larger than after SSWs. This is different to Oehrlein et al. (2020), who reported that the SLP anomalies following SSWs are stronger than that after VIs. Differences in the definition of strong polar vortex events may contribute to this discrepancy. More importantly, however, our model shows that interactive ozone enhances the positive phase of the NAO (Fig. 7h), consistent with the ozone-related extra strengthening of the polar vortex (Fig. 6h).

Finally, returning to Fig. 6, we find that interactive ozone also generates signals in the stratosphere prior to SSW and VI events. For instance, from −60 to −30 days before VI events, the polar vortex is weaker in VARO3 compared to FIXO3 (Fig. 6h), leading to a less positive NAO in VARO3 than in FIXO3 (not shown). The typical reduction in upward directed wave activity that precedes VIs is also weaker in VARO3 than in FIXO3 (Fig. S3), resulting in a reduced acceleration of the polar vortex (Fig. S4). While the reasons for these differences are not fully understood, shortwave radiative processes over the polar cap must be ruled out because, during this time of the year (December–January), there is little to no sunlight over this region. Therefore, the interaction of stratospheric ozone with shortwave radiation and circulation over the lower latitudes is a plausible explanation. A possible mechanism could be the interaction of ozone with planetary waves, which weakens the polar vortex in the middle to lower stratosphere (Albers and Nathan 2012). However, addressing this issue requires additional research and must be left to future studies.

4. Summary and discussion

This study used an idealized general circulation model with a simplified ozone and radiation parameterization to investigate the interaction of ozone with the northern wintertime stratospheric polar vortex. Two long simulations were performed: one in which ozone is allowed to freely evolve and interact with the circulation in dynamically consistent ways (VARO3), and one in which the daily evolving but annually repeating climatological mean ozone distribution of VARO3 is prescribed to the model (FIXO3). The study focused on years with extreme circulation events during February and March, where the polar vortex is either weaker and warmer (SSWs) or stronger and colder (VIs) than normal. By comparing the differences between the two simulations, the importance of interactive ozone was assessed.

Our findings suggest that compared to using fixed ozone, interactive ozone increases the interannual circulation variability of the Arctic stratosphere by 20%–25% during boreal spring (Fig. 1) and prolongs the persistence of the NAM index in the lower stratosphere during boreal spring (Fig. 2). We further found that interactive ozone amplifies the temperature and circulation anomalies that typically follow late-winter SSW and especially VI events during northern spring. This amplification can be attributed to the ozone anomalies, which

are created by the extreme circulation events (SSWs or VIs) during the prior winter (Figs. 3 and 4), persist into spring, and reinforce the temperature (Fig. 5) and circulation anomalies (Fig. 6) of the events. The stronger circulation increases the lifetime of the polar vortex perturbations, extends the persistence time scale of the stratospheric NAM (Fig. 2), and increases the surface impact of the stratospheric circulation events (Fig. 7). Additionally, the increased persistence accounts for the observed rise in interannual U60 variability during spring (Fig. 1) and explains why, after VIs, the mean breakdown date of the polar vortex is delayed by 5 days (Table 1).

The above-described effects are the result of circulation-induced changes in polar ozone. In spring, when there is sufficient sunlight, the changes in ozone create shortwave heating anomalies that reinforce the original anomalies associated with the perturbed polar vortex. Several factors may contribute to the changes in polar ozone:

1) VIs are associated with a decrease in upward planetary wave propagation and dissipation, which stabilizes the polar vortex, weakens the downwelling branch of the BDC, and consequently reduces the transport of ozone-rich air into polar latitudes. Conversely, upward planetary wave propagation is increased before SSWs, disturbing the polar vortex, strengthening the BDC, and increasing the ozone transport into polar latitudes.
2) The reduced (increased) BDC during VIs (SSWs) leads to anomalous adiabatic cooling (warming). By the thermal wind relationship, this creates a dynamical response that further strengthens (weakens) the polar vortex. This reduces (increases) the meridional mixing of polar air with relatively ozone-rich surrounding air, contributing to a further decrease (increase) in polar ozone.
3) The cooling (warming) associated with VIs (SSWs) enhances (decreases) catalytic ozone depletion and further reduces (increases) ozone levels.

The combined changes in ozone create shortwave heating anomalies that reinforce the original temperature and circulation anomalies associated with the perturbed polar vortex. However, we hesitate to label this effect as a positive feedback. The initial driver of the changes in ozone is likely the anomalous transport by the BDC. During VIs, catalytic processes significantly contribute to additional ozone depletion (Tegtmeier et al. 2008). While changes in ozone do amplify the anomalies in polar vortex strength, a true feedback loop would require the vortex anomalies to modify ozone in turn. This could involve additional factors, such as changes in meridional mixing, but we believe that the transport-induced changes in ozone by the BDC in combination with chemical ozone depletion during VIs are the most significant.

The results from our study mostly corroborate and extend findings from similar studies using more complex CCMs. However, we also observed some discrepancies compared to previous studies. For example, we were unable to identify the negative feedback described by Lin et al. (2017) and Haase and Matthes (2019). Further, the perturbed signals in our study were generally weaker than those found in studies using full CCMs, especially at the surface. Some of these differences may stem from our model's simplicity. Most importantly, the Held–Suarez forcing nudges temperatures to observations to mimic the missing physics, which is certainly not fully realistic. The linear ozone scheme relaxes ozone toward a climatology and crudely represents heterogeneous ozone chemistry (Hong and Reichler 2021b), which may lead to large discrepancies between observed and simulated ozone under certain conditions (Monge-Sanz et al. 2022). Further, the model lacks longwave radiative ozone effects. These simplifications likely account for some of the differences between this study and others that use full CCMs, but it is difficult to determine their combined effect on the ozone-circulation interaction.

Nevertheless, this study presents several key take-home messages. Firstly, the SCDM is a valuable tool for studying the fundamental interactions between ozone and stratospheric dynamics. It effectively captures the essential physical principles of these interactions while operating at a fraction of the cost of more complex models. Secondly, our study shows that interactive ozone amplifies the effects of stratospheric circulation anomalies during spring. In contrast, other studies suggest that interactive ozone might moderate these effects. Thirdly, all studies agree that the interaction between ozone and stratospheric circulation has substantial effects and is crucial for climate predictions on subseasonal to multidecadal time scales. Fourthly, the differences between our findings and those of previous studies indicate that there are still significant uncertainties in understanding the ozone–circulation interaction. This underscores the necessity for additional research to reconcile these conflicting results and enhance our understanding of the underlying mechanisms.

Acknowledgments. We thank the National Science Foundation (Grants 1446292 and 2103013), the Department of Atmospheric Sciences at the University of Utah, and the Postdoctoral Scholar Program of the Academia Sinica and the Research Center for Environmental Changes for their support. We also thank the three anonymous reviewers for their constructive comments that helped to improve our manuscript. The use of the computing infrastructure from the Center for High Performance Computing at the University of Utah is gratefully acknowledged.

Data availability statement. The SCDM simulation data can be made available upon request.

REFERENCES

Albers, J. R., and T. R. Nathan, 2012: Pathways for communicating the effects of stratospheric ozone to the polar vortex: Role of zonally asymmetric ozone. *J. Atmos. Sci.*, **69**, 785–801, https://doi.org/10.1175/JAS-D-11-0126.1.

Baldwin, M. P., and T. J. Dunkerton, 2001: Stratospheric harbingers of anomalous weather regimes. *Science*, **294**, 581–584, https://doi.org/10.1126/science.1063315.

Bosilovich, M. G., and Coauthors, 2015: MERRA-2: Initial evaluation of the climate. NASA Tech. Memo. NASA/TM-2015-104606/

Vol.43, 145 pp. https://gmao.gsfc.nasa.gov/reanalysis/MERRA-2/docs/.

Butchart, N., 2014: The Brewer-Dobson circulation. *Rev. Geophys.*, **52**, 157–184, https://doi.org/10.1002/2013RG000448.

Cariolle, D., and H. Teyssèdre, 2007: A revised linear ozone photochemistry parameterization for use in transport and general circulation models: Multi-annual simulations. *Atmos. Chem. Phys.*, **7**, 2183–2196, https://doi.org/10.5194/acp-7-2183-2007.

Charlton, A. J., and L. M. Polvani, 2007: A new look at stratospheric sudden warmings. Part I: Climatology and modeling benchmarks. *J. Climate*, **20**, 449–469, https://doi.org/10.1175/JCLI3996.1.

Charney, J. G., and P. G. Drazin, 1961: Propagation of planetary-scale disturbances from the lower into the upper atmosphere. *J. Geophys. Res.*, **66**, 83–109, https://doi.org/10.1029/JZ066i001p00083.

Cicerone, R. J., 1987: Changes in stratospheric ozone. *Science*, **237**, 35–42, https://doi.org/10.1126/science.237.4810.35.

Compo, G. P., and Coauthors, 2011: The twentieth century reanalysis project. *Quart. J. Roy. Meteor. Soc.*, **137**, 1–28, https://doi.org/10.1002/qj.776.

de la Cámara, A., M. Abalos, P. Hitchcock, N. Calvo, and R. R. Garcia, 2018: Response of Arctic ozone to sudden stratospheric warmings. *Atmos. Chem. Phys.*, **18**, 16 499–16 513, https://doi.org/10.5194/acp-18-16499-2018.

Friedel, M., G. Chiodo, A. Stenke, D. I. V. Domeisen, and T. Peter, 2022: Effects of Arctic ozone on the stratospheric spring onset and its surface impact. *Atmos. Chem. Phys.*, **22**, 13 997–14 017, https://doi.org/10.5194/acp-22-13997-2022.

Gabriel, A., D. Peters, I. Kirchner, and H.-F. Graf, 2007: Effect of zonally asymmetric ozone on stratospheric temperature and planetary wave propagation. *Geophys. Res. Lett.*, **34**, L06807, https://doi.org/10.1029/2006GL028998.

Gillett, N. P., and D. W. J. Thompson, 2003: Simulation of recent Southern Hemisphere climate change. *Science*, **302**, 273–275, https://doi.org/10.1126/science.1087440.

Haase, S., and K. Matthes, 2019: The importance of interactive chemistry for stratosphere–troposphere coupling. *Atmos. Chem. Phys.*, **19**, 3417–3432, https://doi.org/10.5194/acp-19-3417-2019.

——, J. Fricke, T. Kruschke, S. Wahl, and K. Matthes, 2020: Sensitivity of the Southern Hemisphere circumpolar jet response to Antarctic ozone depletion: Prescribed versus interactive chemistry. *Atmos. Chem. Phys.*, **20**, 14 043–14 061, https://doi.org/10.5194/acp-20-14043-2020.

Hartmann, D. L., 1981: Some aspects of the coupling between radiation, chemistry, and dynamics in the stratosphere. *J. Geophys. Res.*, **86**, 9631–9640, https://doi.org/10.1029/JC086iC10p09631.

Harzer, F., H. Garny, F. Ploeger, H. Bönisch, P. Hoor, and T. Birner, 2023: On the pattern of interannual polar vortex–ozone co-variability during Northern Hemispheric winter. *Atmos. Chem. Phys.*, **23**, 10 661–10 675, https://doi.org/10.5194/acp-23-10661-2023.

Held, I. M., 2005: The gap between simulation and understanding in climate modeling. *Bull. Amer. Meteor. Soc.*, **86**, 1609–1614, https://doi.org/10.1175/BAMS-86-11-1609.

——, and M. J. Suarez, 1994: A proposal for the intercomparison of the dynamical cores of atmospheric general circulation models. *Bull. Amer. Meteor. Soc.*, **75**, 1825–1830, https://doi.org/10.1175/1520-0477(1994)075<1825:APFTIO>2.0.CO;2.

Hersbach, H., and Coauthors, 2018: Operational global reanalysis: Progress, future directions and synergies with NWP. ERA Rep. 27, 65 pp., https://doi.org/10.21957/tkic6g3wm.

——, and Coauthors, 2020: The ERA5 global reanalysis. *Quart. J. Roy. Meteor. Soc.*, **146**, 1999–2049, https://doi.org/10.1002/qj.3803.

Hocke, K., M. Lainer, and A. Schanz, 2015: Composite analysis of a major sudden stratospheric warming. *Ann. Geophys.*, **33**, 783–788, https://doi.org/10.5194/angeo-33-783-2015.

Hong, H.-J., and T. Reichler, 2021a: Local and remote response of ozone to Arctic stratospheric circulation extremes. *Atmos. Chem. Phys.*, **21**, 1159–1171, https://doi.org/10.5194/acp-21-1159-2021.

——, and ——, 2021b: The Simplified Chemistry-Dynamical Model (SCDM V1.0). *Geosci. Model Dev.*, **14**, 6647–6660, https://doi.org/10.5194/gmd-14-6647-2021.

Hu, J., R. Ren, and H. Xu, 2014: Occurrence of winter stratospheric sudden warming events and the seasonal timing of spring stratospheric final warming. *J. Atmos. Sci.*, **71**, 2319–2334, https://doi.org/10.1175/JAS-D-13-0349.1.

Ivanciu, I., K. Matthes, S. Wahl, J. Harlaß, and A. Biastoch, 2021: Effects of prescribed CMIP6 ozone on simulating the Southern Hemisphere atmospheric circulation response to ozone depletion. *Atmos. Chem. Phys.*, **21**, 5777–5806, https://doi.org/10.5194/acp-21-5777-2021.

Keeble, J., and Coauthors, 2021: Evaluating stratospheric ozone and water vapour changes in CMIP6 models from 1850 to 2100. *Atmos. Chem. Phys.*, **21**, 5015–5061, https://doi.org/10.5194/acp-21-5015-2021.

Kidston, J., A. A. Scaife, S. C. Hardiman, D. M. Mitchell, N. Butchart, M. P. Baldwin, and L. J. Gray, 2015: Stratospheric influence on tropospheric jet streams, storm tracks and surface weather. *Nat. Geosci.*, **8**, 433–440, https://doi.org/10.1038/ngeo2424.

Kim, J., and T. Reichler, 2016: Quantifying the uncertainty of the annular mode time scale and the role of the stratosphere. *Climate Dyn.*, **47**, 637–649, https://doi.org/10.1007/s00382-015-2860-2.

Lacis, A. A., and J. Hansen, 1974: A parameterization for the absorption of solar radiation in the Earth's atmosphere. *J. Atmos. Sci.*, **31**, 118–133, https://doi.org/10.1175/1520-0469(1974)031<0118:APFTAO>2.0.CO;2.

Li, F., Y. V. Vikhliaev, P. A. Newman, S. Pawson, J. Perlwitz, D. W. Waugh, and A. R. Douglass, 2016: Impacts of interactive stratospheric chemistry on Antarctic and Southern Ocean climate change in the Goddard Earth Observing System, version 5 (GEOS-5). *J. Climate*, **29**, 3199–3218, https://doi.org/10.1175/JCLI-D-15-0572.1.

Limpasuvan, V., D. W. J. Thompson, and D. L. Hartmann, 2004: The life cycle of the Northern Hemisphere sudden stratospheric warmings. *J. Climate*, **17**, 2584–2596, https://doi.org/10.1175/1520-0442(2004)017<2584:TLCOTN>2.0.CO;2.

——, D. L. Hartmann, D. W. J. Thompson, K. Jeev, and Y. L. Yung, 2005: Stratosphere-troposphere evolution during polar vortex intensification. *J. Geophys. Res.*, **110**, D24101, https://doi.org/10.1029/2005JD006302.

Lin, P., D. Paynter, L. Polvani, G. J. P. Correa, Y. Ming, and V. Ramaswamy, 2017: Dependence of model-simulated response to ozone depletion on stratospheric polar vortex climatology. *Geophys. Res. Lett.*, **44**, 6391–6398, https://doi.org/10.1002/2017GL073862.

Lubis, S. W., V. Silverman, K. Matthes, N. Harnik, N.-E. Omrani, and S. Wahl, 2017: How does downward planetary wave coupling affect polar stratospheric ozone in the Arctic winter stratosphere? *Atmos. Chem. Phys.*, **17**, 2437–2458, https://doi.org/10.5194/acp-17-2437-2017.

Manney, G. L., and Coauthors, 2011: Unprecedented Arctic ozone loss in 2011. *Nature*, **478**, 469–475, https://doi.org/10.1038/nature10556.

——, and Coauthors, 2020: Record-low Arctic stratospheric ozone in 2020: MLS observations of chemical processes and comparisons with previous extreme winters. *Geophys. Res. Lett.*, **47**, e2020GL089063, https://doi.org/10.1029/2020GL089063.

McCormack, J. P., S. D. Eckermann, D. E. Siskind, and T. J. McGee, 2006: CHEM2D-OPP: A new linearized gas-phase ozone photochemistry parameterization for high-altitude NWP and climate models. *Atmos. Chem. Phys.*, **6**, 4943–4972, https://doi.org/10.5194/acp-6-4943-2006.

Monge-Sanz, B. M., and Coauthors, 2022: A stratospheric prognostic ozone for seamless Earth system models: Performance, impacts and future. *Atmos. Chem. Phys.*, **22**, 4277–4302, https://doi.org/10.5194/acp-22-4277-2022.

Nathan, T. R., and E. C. Cordero, 2007: An ozone-modified refractive index for vertically propagating planetary waves. *J. Geophys. Res.*, **112**, D02105, https://doi.org/10.1029/2006JD007357.

Oehrlein, J., G. Chiodo, and L. M. Polvani, 2020: The effect of interactive ozone chemistry on weak and strong stratospheric polar vortex events. *Atmos. Chem. Phys.*, **20**, 10 531–10 544, https://doi.org/10.5194/acp-20-10531-2020.

Rae, C. D., J. Keeble, P. Hitchcock, and P. A. Pyle, 2019: Prescribing zonally asymmetric ozone climatologies in climate models: Performance compared to a chemistry-climate model. *J. Adv. Model. Earth Syst.*, **11**, 918–933, https://doi.org/10.1029/2018MS001478.

Randel, W. J., and F. Wu, 1999: Cooling of the Arctic and Antarctic polar stratospheres due to ozone depletion. *J. Climate*, **12**, 1467–1479, https://doi.org/10.1175/1520-0442(1999)012<1467:COTAAA>2.0.CO;2.

Revell, L. E., F. Robertson, H. Douglas, O. Morgenstern, and D. Frame, 2022: Influence of ozone forcing on 21st century Southern Hemisphere surface westerlies in CMIP6 models. *Geophys. Res. Lett.*, **49**, e2022GL098252, https://doi.org/10.1029/2022GL098252.

Rieder, H. E., G. Chiodo, J. Fritzer, C. Wienerroither, and L. M. Polvani, 2019: Is interactive ozone chemistry important to represent polar cap stratospheric temperature variability in Earth-system models? *Environ. Res. Lett.*, **14**, 044026, https://doi.org/10.1088/1748-9326/ab07ff.

Romanowsky, E., and Coauthors, 2019: The role of stratospheric ozone for Arctic-midlatitude linkages. *Sci. Rep.*, **9**, 7962, https://doi.org/10.1038/s41598-019-43823-1.

Rupp, P., J. Spaeth, H. Garny, and T. Birner, 2023: Enhanced polar vortex predictability following sudden stratospheric warming events. *Geophys. Res. Lett.*, **50**, e2023GL104057, https://doi.org/10.1029/2023GL104057.

Saha, S., and Coauthors, 2014: The NCEP Climate Forecast System version 2. *J. Climate*, **27**, 2185–2208, https://doi.org/10.1175/JCLI-D-12-00823.1.

Solomon, S., 1999: Stratospheric ozone depletion: A review of concepts and history. *Rev. Geophys.*, **37**, 275–316, https://doi.org/10.1029/1999RG900008.

Stolarski, R. S., and R. J. Cicerone, 1974: Stratospheric chlorine: A possible sink for ozone. *Can. J. Chem.*, **52**, 1610–1615, https://doi.org/10.1139/v74-233.

Tegtmeier, S., M. Rex, I. Wohltmann, and K. Krüger, 2008: Relative importance of dynamical and chemical contributions to Arctic wintertime ozone. *Geophys. Res. Lett.*, **35**, L17801, https://doi.org/10.1029/2008GL034250.

——, V. E. Fioletov, and T. G. Shepherd, 2010: A global picture of the seasonal persistence of stratospheric ozone anomalies. *J. Geophys. Res.*, **115**, D18119, https://doi.org/10.1029/2009JD013011.

Thompson, D. W. J., and S. Solomon, 2002: Interpretation of recent Southern Hemisphere climate change. *Science*, **296**, 895–899, https://doi.org/10.1126/science.1069270.

Wallace, J. M., and P. V. Hobbs, 2006: *Atmospheric Science: An Introductory Survey*. Elsevier Academic Press, 483 pp.

Wu, Z., and T. Reichler, 2018: Towards a more Earth-like circulation in idealized models. *J. Adv. Model. Earth Syst.*, **10**, 1458–1469, https://doi.org/10.1029/2018MS001356.